Synthesis of Circular Double-Stranded DNA Having Single-Stranded Recognition Sequence as molecular-Physical Probe for Nucleic Acid Hybridization Detection Based on Atomic Force microscopy Imaging

Nakano, Koji
Department of Applied Chemistry, Faculty of Engineering, Kyushu University

Matsunaga, Hideshi
Department of Applied Chemistry, Faculty of Engineering, Kyushu University

Murata, Masaharu
Department of Advanced Medical Initiatives, Faculty of Medical Sciences, Kyushu University

Soh, Nobuaki
Department of Applied Chemistry, Faculty of Engineering, Kyushu University

他

出版情報：Analytical Sciences. 25 (8), pp.993-998, 2009-08-10. 公益社団法人日本分析化学会
バージョン：

ANALYTICAL SCIENCES AUGUST 2009, VOL. 25

Synthesis of Circular Double-Stranded DNA Having Single-Stranded Recognition Sequence as Molecular-Physical Probe for Nucleic Acid Hybridization Detection Based on Atomic Force Microscopy Imaging

Koji NAKANO,*† Hideshi MATSUNAGA,* Masaharu MURATA, Nobuaki SOH,* and Toshihiko IMATO***

**Department of Applied Chemistry, Faculty of Engineering, Kyushu University, 744 Motooka, Nishi, Fukuoka 819-0395, Japan*
***Department of Advanced Medical Initiatives, Faculty of Medical Sciences, Kyushu University, 3-1-1 Maidashi, Higashi, Fukuoka 812-8582, Japan*

A new class of DNA probes having a mechanically detectable tag is reported. The DNA probe, which consists of a single-stranded recognition sequence and a double-stranded circular DNA entity, was prepared by polymerase reaction. M13mp18 single strand and a 32mer oligodeoxynucleotide whose 5′-end is decorated with the recognition sequence were used in combination as template and primer, respectively. We have successfully demonstrated that the DNA probe is useful for bioanalytical purposes: by deliberately attaching target DNA molecules onto Au(111) substrates and by mechanically reading out the tag-entity using a high-resolution microscopy including atomic force microscopy, visualization/detection of the individual target/probe DNA conjugate was possible simply yet straightforwardly. The present DNA probe can be characterized as a 100%-nucleic acid product material. It is simply available by one-pod synthesis. A surface topology parameter, image roughness, has witnessed its importance as a quantitative analysis index with particular usability in the present visualization/detection method.

(Received February 26, 2009; Accepted April 2, 2009; Published August 10, 2009)

Introduction

DNA sensing has involved chemical modifications of either the capture probe DNA or the target DNA with small molecules, which are capable of reporting the molecular recognition events. Fluorophores are the best-established materials, as manifested in, *e.g.*, the Sanger method of DNA sequencing and in the high-throughput gene analysis applications using DNA chips/microarrays.[1,2] Researchers motivated by recent nanotechnology developments, on the other hand, have examined various nanoparticle tags including gold,[3-5] silver,[6] quantum dots,[7,8] and polymers[9] in a combined use of a variety of chemical or physical measurements. Among them, for visualization measurement/detection purposes, atomic force microscopy (AFM) studies should be interesting.[10] A higher lateral resolution of AFM down to single-nanoparticle-level allows, in principle, the direct detection of individual DNA-hybridization events between the surface-confined capture probe DNA and the target DNA dissolved in the solution phase.

We have previously reported chemically modified electrodes from glucose oxidase,[11] cytochrome *c*,[12] and plasmid DNA[13] in which we have successfully obtained AFM images for the particular biomacromolecules down to single-molecular resolution. These achievements, along with the fulfillment of the DNA biosensor requrements,[14] led us to investigate a new DNA probe, with which the read-out of the DNA-hybridization event become possible by simply imaged by AFM. We have designed a DNA probe that consists of a recognition sequence and a reporting portion, which can develop a particular superstructure with steric bulk. For the purpose, we took advantage of enzymic replication of a single-stranded, circular DNA with using a new class of primer DNA, which possesses an excess sequence at the 5′-position as a "decoration". With simple polymerase reaction at the template DNA, we anticipated a double-stranded, circular DNA leaving the specific decorate portion unreplicated. This single-stranded sequence can potentially recognize the target DNAs that contain complementary sequences and bind to them, *i.e.*, the DNA thus synthesized acts as a kind of ligand to the target DNA. When one deliberately modifies a substrate surface with the target DNA, the individual DNA conjugate thus formed can be simply yet straightforwardly imaged by AFM to detect the hybridization event.

In the present paper, we will describe the synthesis and characterization of a new DNA probe (DNA ligand) that possesses both the molecular recognition capability and the mechanical functionality required (Scheme 1). We set a single-stranded vector DNA (M13mp18) as the template while the decorated primer contains, as a model system, the K-ras 12 gene whose mutations are presented in greater than 50% of colorectal adenomas and carcinomas. With the higher spatial resolving power that AFM provides, a DNA hybridization assay based on visualization/detection method for the individual DNA

† To whom correspondence should be addressed.
E-mail: kojitcm@mbox.nc.kyushu-u.ac.jp

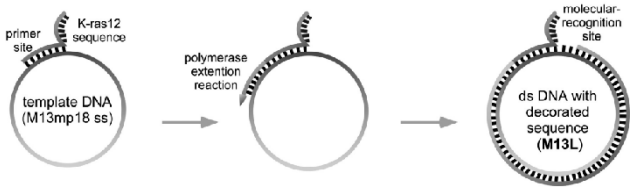

Scheme 1 Preparation of a double-stranded circular DNA probe molecule with a hybridization capable single-stranded recognition sequence.

conjugate molecule was successfully demonstrated. Effects of DNA mismatch on the hybridization/adsorption at the substrate surface were also investigated and are discussed in detail, based the results obtained for a series of control DNA ligands and target sequences.

Experimental

Reagents and chemicals

For the probe DNA synthesis, M13mp18 single strand DNA (7249 base) was used for the template and replication was made by Takara Ex Taq® polymerase using dNTP mixture as the substrate. They were purchased from Takara Bio Inc. and were used as received. For the purification of the reaction product, Microcon® centrifugal filter units were used (YM-50, Millipore). Restriction enzyme digestion of the circular DNA was made using *Hin*d III, Takara Bio Inc. Streptavidin was purchased from Sigma-Aldrich Japan K. K. Other chemicals were guaranteed reagents and were used as received.

The oligonucleotides used in the present study including two-types of the primer sequence (**pr1** and **pr2**), and four-kinds of the target DNAs in 3′-biotinylated form, all of which were custom-synthesized by the supplier (Sigma-Aldrich Japan K. K.) and were used as received. They are shown below.

pr 1 5′-GGA GCT GGT GGC-TTT TTT TTT T-GG **GAA TTC** GTA ATC ATG GTC-3′

pr 2 5′-TTT TTT TTT T-GG **GAA TTC** GTA ATC ATG GTC-3′

complementary strand	5′-GCC ACC AGC TCC-biotin-3′
scramble strand	5′-ATT GTT GAT CTT-biotin-3′
1-mismatch strand (**m1**)	5′-GCC ACC **T**GC TCC-biotin-3′
3-mismatch strand (**m3**)	5′-GCC **T**CC **T**GC **A**CC-biotin-3′

Template synthesis of DNA probe

A 20-μL portion of M13mp18 single strand DNA (0.1 μM) was mixed with 100 μM-primer (**pr1**) solution (2 μL), 10 × PCR buffer (3 μL), 2.5 mM-dNTP solution (2 μL), and 5U/μL-*Taq* polymerase solution (2 μL). After a 1 μL-portion of sterile water was added to give a 30-μL solution, the reaction mixture was first denatured at 95°C for 5 min and then was annealed at 55°C for 5 min. Subsequently, the polymerase reaction was allowed to proceed at 72°C for 2 h. After the reaction, the product mixture was extracted by phenol/chloroform, followed by ethanol precipitation. The probe DNA thus obtained was further purified by ultrafiltration using Microcon® centrifugal filter units at 3000 rpm. For control experiments, a replication reaction using **pr2** was also done and the double-stranded form of M13mp18 without the adhesive sequence was obtained. Agarose gel electrophoresis was made to confirm that the replication of the template DNA was completed. The reaction product was first digested by *Hin*d III and was electromigrated on a 9%-agarose gel in TEA buffer (pH 8.1) at 100 V for 30 min. UV illumination of the ethidium bromide stained gel gave the migration profile.

AFM imaging

A Nanoscope IV controller equipped with a MultiMode AFM unit, both of which were products from Veeco Metrology Inc., was used throughout of the study. Tapping mode AFM using an NCH-10V cantilever (Veeco Metrology Inc.) collected the topological image for the probe DNA that was electrostatically attached onto mica surfaces using Mg^{2+}-crosslinking method[15] at an ambient atmosphere and temperature (25°C). In the hybridization/adsorption assay experiments, avidin-biotin chemistry was used for target DNA immobilization.[16] Evaporated gold films having (111) texture (1 × 1 cm, Agilent Technologies, Inc.) were first annealed in a hydrogen flame to reconstruct the surface. The substrate was immediately immersed into a streptavidin solution (0.2 mg/cm^3 in PBS) for 10 min and then was rinsed thoroughly with PBS, followed by sterile water. Atop the substrate surface was cast the target DNA solution (0.2 mg/cm^3 in PBS) and the substrate was settled in an airtight vessel which was maintained at saturated humidity to prevent dryness. The surface affinity complexes were allowed to form for 20 min at an ambient temperature (25°C). Finally, the substrate was rinsed thoroughly with PBS, followed by sterile water, then dried under a reduced pressure for 1 h. Tapping mode AFM imaged the substrate surface phase thus formed. In case of hybridization experiments, the Au substrate having the target-DNA/protein/Au interfacial structure was treated by a 5-μL portion of the ligand DNA solution (0.2 mg/cm^3 in PBS) in an airtight vessel for 20 min, under saturated humidity and at an ambient temperature (25°C). AFM imaging was done by the procedure described above.

Results and Discussion

Probe design, synthesis, and characterization

As mentioned previously, with the help of high-resolution microscopy methods including AFM, DNA probes with a mechanical tag have been showing their potential capability as label-free methods in DNA hybridization analysis. Nanoparticles have been used as the tag matters due to their favorable size for microscopy imaging. On the other hand, DNA has been spotlighted as polymeric biomaterials in nanometer-scale architecture synthesis, *i.e.*, DNA origami.[17] With rational higher-order structure developments, a DNA probe molecule can be used, by itself, for such types of hybridization assay. A circular structure seen in plasmid DNAs should be the primary choice, since such a distinct spatial configuration is imaged by AFM straightforwardly.

Previously, Nakagami and coworkers reported a circular DNA probe that consists of two single-stranded DNAs.[18] They independently prepared and hybridized two kinds of single-stranded plasmid DNAs: into one of the strands is cloned the complementary sequence to a target gene while the other was modified with small-molecule tags. In contrast, our probe design relies on a simpler approach: a primer DNA that contains an extra sequence complementary to the target gene (underlined

Fig. 1 Agarose gel electrophoresis profiles for the polymerase reaction products after *Hin*d III digestion. Lane: 1, λDNA; 2, **M13L**; 3, **M13D**; 4, M13mp18 RF DNA.

sequence) is introduced into the polymerase reaction on a single-stranded circular template DNA. The decorating sequence that protrudes forward facing the nucleotide-extension direction will inevitably hinder the reaction to form unreplicated, single-stranded portions. However, we can expect that the decorating portion of the primer sequence has little effect in replication of the template on the analogy of the rolling-circular amplification method which can produce a long single-stranded product DNA.[19] Also, in an earlier study on unwinding of DNA duplex by a helicase-primase enzymic reaction, we can see an example of this types of polymerase extension reaction.[20] The determination of the extent of the nucleobases left unreplicated should be the challenges for the future studies. Finally, as the primer site (doubly underlined portion), we chose the 20mer sequence including *Eco*R I site (**GAA TTC**) in M13mp18 vector DNA. Hereafter, we will denote the DNA probe having ligand ability as **M13L**. We made the template reaction using **pr2**, which does not contain the recognition sequence and thus yields the binding-silent double-stranded form denoted as **M13D**.

As shown in Fig. 1, in agarose gel electrophoretic analysis, both **M13L** and **M13D** in the scissioned, linear form gave a band at around 7000 bp. Furthermore, the control experiment on the linearized M13mp18 phage vector DNA (7249 bp) was found to possess almost the same gel retardation migration. The electrophoresis profile is additionally characterized with a delicate feature having a little greater mobility: this should be ascribed to the impurity fragments due to the limited purity of the DNA sample (70%). Obtaining these results, we can conclude that the polymerase reaction described here can convert the template DNA to the corresponding double-stranded form.

The UV spectrum for **M13L** in PBS is shown in Fig. 2. We found that it was a common practice to perform a quick assessment of the purity of nucleic acid samples; the A_{260} over A_{280} ratio is greater than 2. However, one can see that its irregular shape showing two shoulders at 275 and 265 nm characterizes the spectrum, which is indicative of a mixture of proteins. Since the primary concern of the AFM imaging is the topological nature of the target, impurity components such as proteins, affect the reliability of analysis significantly. Although the method of DNA purification remains to be solved in the future, we met lower effects of impurity protein in the AFM assay as shown in the following section.

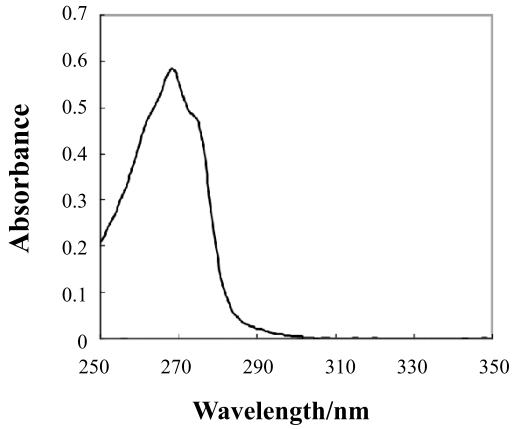

Fig. 2 UV absorption spectrum of **M13L** dissolved in TE buffer.

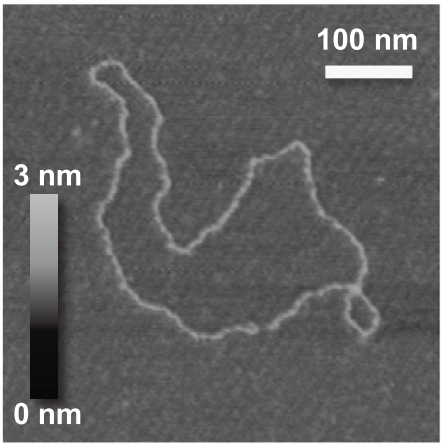

Fig. 3 AFM image for **M13L** electrostatically attached on mica surface.

Lastly, we made simple AFM observations of the probe DNA electrostatically attached on mica surfaces. Shown in Fig. 3 is a representative AFM image of **M13L**. It is apparent that the DNA probe has open-circular conformation, as anticipated. The measured averaged width and heights were 8.9 ± 0.6 nm and 0.58 ± 0.06 nm, respectively; both of them were consistent to those seen in the literature data.[15] Such results positively evidenced the double-helical form. One may notice that, in the bottom part of the substance, a thinner drawn, very fine structure connects the entire circular structure. The particular structure was estimated to be 14 nm in length, which should be equivalent to 45 nucleobase-pairs. This segment most probably represents the single-stranded part of the template DNA. However, we have not yet reliably evidenced the structural details. More information will hereafter be described in detail.

Hybridization assay and AFM visualization/detection

In Fig. 4 we summarize the AFM images obtained with a series of **M13L** hybridization/adsorption experiments. As seen in image (a), for the Au substrate in the unmodified state, the surface phase can be characterized with atomically flat, terrace structures that originate from the (111) crystal face being exposed. After the target-DNA/protein conjugate adlayer formation, the surface gave images very different from the bare, initial state (Fig. 4b): although some aggregated domains are partially observed, compact spherical bodies are finely

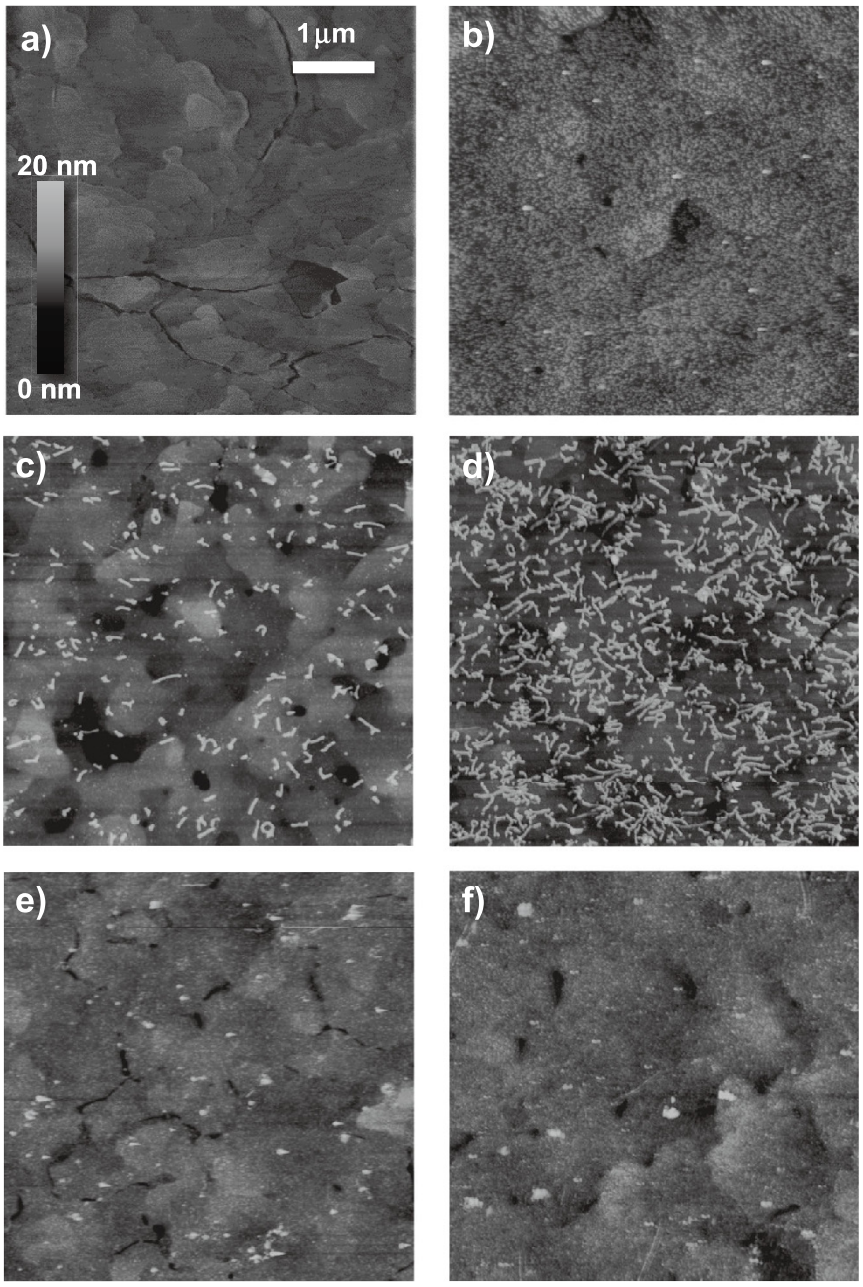

Fig. 4 Detection of individual **M13L** molecule adsorbed through hybridization at the target-DNA confined substrate surface. Results of a series of AFM imaging are shown for the bare Au(111) substrate (a), after the target-DNA/protein adlayer formation (b), and the same substrates treated with the **M13L** solution (c). For comparison, results for the hybridization experiment of the Au(111) with the target-DNA/protein interfacial structure using the **M13L** solution with 1000-times higher concentration (d), M13mp18 single strand DNA (e), and **M13D** (f) are also shown.

distributed covering the substrate surface almost completely. Each spheroid must be an individual conjugate molecule. The displays of atomically flat Au(111) grains with ill-defined step edges should be indicative of self-assembly of the adsorbate molecules to form well-packed, uniform surface adlayers. Meanwhile the Au substrate gave almost the same surface topological image only when the exposure to the protein solution was made (data not shown).

Treatments of the Au substrate with the **M13L** solution further transformed the adlayer structure, producing distinct differences in its surface state (Fig. 4c): while the surface spherical bodies diminishes almost completely, many surface matters appeared. Most of them have a rod-like shape of 43 ± 1.8 nm in width and 6.3 ± 0.26 nm in height ($n = 25$). In AFM experiments, observing more than one entity having significant differences in height generally lowers the z-direction resolution; this should result in each surface spheroid observed in Fig. 4b becoming unresolved in the particular AFM image. On the other hand, the newly observed surface substances must be individual **M13L** molecules: when we made the same experiments using a **M13L** solution of 1000-times higher in concentration, we observed the rod-like matters that develop surface adlayers to cover almost whole surface (Fig. 4d). They remained entirely adsorbed after rinsing with PBS solution, showing that this type of

immobilization occurred not electrostatically but in a bioaffinity manner, *i.e*. hybridization of nucleobases-pairs as designed. Here, it should be pointed out that **M13L** molecules possess tightly packed coagulated structures that are totally different from the circular conformer (Fig. 3). The structural transformation should be addressed as follows. At the mica surface, **M13L** is electrostatically attached with the entire DNA-chain surface that interacts at the mica anionic sites *via* Mg^{2+}, leading the double-helical DNA to freeze almost completely. In cases of hybridization adsorption of **M13L**, immobilizations are forced only by the single-stranded site to bind to the surface-confined target-DNA and thus allow the conjugate molecule to freely change its conformation even after immobilization. For the linear-shaped conformers observed in AFM images, contour length measurements determined the specific length to be 214 ± 31 nm (n = 20). Since one nucleotide unit is 0.33 nm long, the base-number for the template (7249) simply indicates the specific molecular length for **M13L** to be 2392 nm. Comparing those, the rod-like structures may represent a 10-times-folded conformer from the **M13L** DNA duplex. On the other hand, it is commonly accepted that the finite dimensions of the cantilever tips induce lateral deformation of the object imaged, including DNA. Thus, the apparent height in an AFM image, rather than the apparent width, can more reliably report the molecular dimension of the object since it is potentially free from the structural deformation.[15] The molecular height data for **M13L** (Fig. 3) again gives the same folding number of 10 when compared with that for the DNA rod entities. These results should strengthen the idea that the simply folded DNA conformers are formed at the surface.

As control, we have further examined the hybridization-adsorption behavior for the template DNA (Fig. 4e), as well as the binding-silent form of the ligand DNA (**M13D**, Fig. 4f). As shown in these figures, neither template DNA nor **M13D** gave any positive indication in the hybridization-adsorption experiments. Although some coagulated grains having a few tenth nm heights are noticed in the AFM images, most probably they are electrolyte salts deposited from the solution phase. Ebersole and coworkers reported that the avidin-biotin chemistry attained a surface concentration of 1.4×10^{-11} mol cm^{-2}.[16] Regarding the amount of sample required, the experiments made here follow substoichiometric conditions; roughly estimated, the present method only requires 2.0×10^{-13} mol cm^{-2} of the probe molecule to be visualized/detected when we take, for instance, the experimental conditions in Fig. 4c. If we adopt a stoichiometrically equivalent concentration condition by reducing the amount of the target DNA to be immobilized at the substrate surface, the straightforwardness of detection attained by visualizing of the individual target-DNA/probe-DNA conjugate should achieve greater sensitivity as a solid-phase hybridization assay method in the near future.

As another control, we have examined the effect of mismatch in the visualization/detection assay. Here we chose three-types of control samples including a scramble sequence, and a target DNA containing 1-mismatch (bold indication) or 3-mismatch. Each sample was attached on the Au substrates in the same fashion and tested following the hybridization/adsorption protocol. As seen in Fig. 5, it is apparent that none of them gave any hybridization/adsorption response. In the case of 1-mismatched sample DNA, one may notice a couple of **M13L** conjugates located at the surface but only rarely. Obtaining these results, we can conclude that the present DNA probe can recognize the target-DNA molecules to bind with them through selective hydrogen bonds that the complementary base pairs can provide.

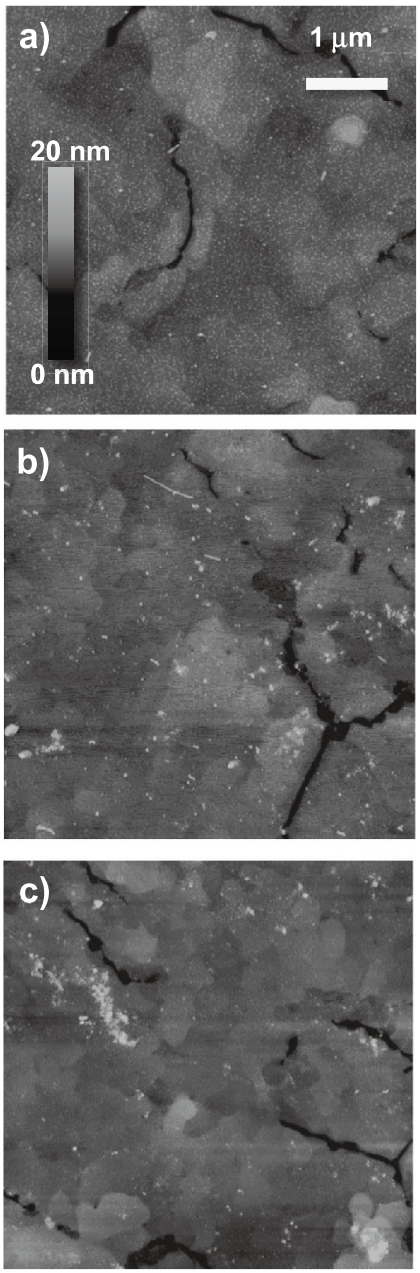

Fig. 5 Representative AFM images for the control experiments. Hybridization experiments were made using **M13L** with the Au(111) substrate having the scramble-DNA/protein (a), **m1**-DNA/protein (b), and **m3**-DNA/protein (c) interfacial structures.

Approaches of semi-quantitative assessment of hybridization-adsorption response

Finally, we will describe a preliminary result of quantification of the present method of solid-phase hybridization assay. Since the AFM images obtained here consist of 512 × 512 pixels, into which the particular height data are encoded, simple arithmetic dot-by-dot treatment can offer a series of single-particle-related topology parameters involving bearing, depth, roughness, and also particle size. On the other hand, determining traditional surface parameters such as roughness factor requires further topology data of the surface. From the exploratory analyses for the AFM images, we found that image roughness, R_a is conveniently applicable and importantly, it does not require any homogeneity in size and shape for the surface-attached

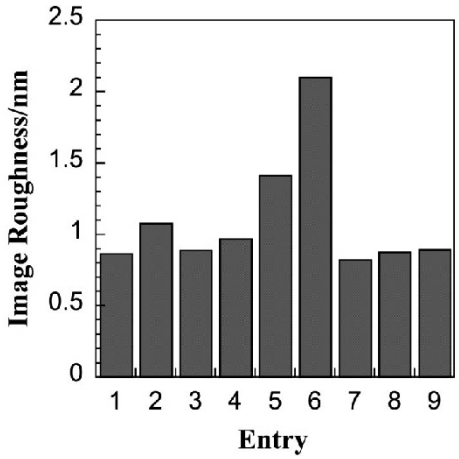

Fig. 6 Comparison of the value of the image roughness determined for the Au substrate after various surface treatment experiments. Entries: 1, bare Au(111) substrate; 2, after the target-DNA/protein adlayer formation; 3, after treatment with M13mp18 single strand; 4, after treatment with **M13D**; 5, after treatment with **M13L**; 6, after treatment with **M13L** solution of 1000-times higher concentration; 7, control experiments of **M13L** hybridization-adsorption for the Au(111) substrate with scramble-DNA/protein interfacial structure; 8, control experiment using the **m1**-DNA/protein/Au substrate; 9, control experiment using the **m3**-DNA/protein/Au substrate.

substances. Image roughness is simply determined by the arithmetic average of the absolute values of the surface height (Z) for the complete pixel data set ($N = 512 \times 512$) and is defined as follows:

$$R_a = \frac{1}{N}\sum_{j=1}^{N}|Z_j|. \quad (1)$$

Results of roughness analysis for the particular AFM images as referred to above are summarized in Fig. 6.

We confirmed that, as one of the underlying premises, all of the substrates commonly gave numerically zero-nm as a mean value for the height data contained within the particular AFM image. Thus, R_a value determined should be simply equivalent with the number average height when the specific height for the surface bodies is almost constant. As seen in Fig. 6, variation of R_a has quantitatively firmed up the discussions. Only the hybridization/adsorption experiments with **M13L** upon target-DNA-confined substrate definitely gave rise to values of R_a having certain concentration dependence. It is apparent that R_a produces no meaningful response toward other target-probe assortments including the bare Au and the **M13L**-untreated Au substrates. Furthermore, R_a can be expected to go up in proportion to the number of the surface entities. Thus, detailed experiments with varying concentration of the probe as well as the surface-confined target DNA will draw a solid foundation for the present method in quantitative analytical purposes in the future.

In conclusion, we have developed a mechanically tagged DNA probe molecule. The new-class of molecule consists of a single-stranded recognition sequence and a double-stranded circular entity, which can bind to the target DNA to be imaged and/or detected by a high-resolution microscopy such as AFM. By taking advantage of a primer sequence whose 5′-end is modified with the recognition sequence, we were able to prepare a DNA probe, in one-pod synthesis manner, by a polymerase reaction at a template DNA. We have successfully demonstrated that visualization/detection for the individual target/probe DNA conjugate is possible with a higher spatial resolution that AFM provides. Although the present method tended to suffer from contamination from experimentation environment, it has shown its significance as a simple yet robust DNA-hybridization assay application. As one of the basic surface topology parameters in AFM, image roughness has showed its importance in quantitative analyses for the future.

Acknowledgements

This work was supported by the Precursory Research for Embryonic Science and Technology of the Japan Science and Technology Agency. We also acknowledge for the financial supports by a Grant-in-Aid for Scientific Research and by Nanotechnology Network Project (Kyushu-area Nanotechnology Network) both of which come from the Ministry of Education, Culture, Sports, Science and Technology (MEXT), Japan.

References

1. M. J. O'Donnell and L. W. McLaughlin, "*Bioorganic Chemistry. Nucleic Acids*", ed. S. M. Hecht, **1996**, Chap. 8, Oxford University Press, New York, 216.
2. A. Manz, N. Pamme, and D. Iossifidis, "*Bioanalytical Chemistry*", **2004**, Chaps. 5 – 6, Imperial College Press, London, 109.
3. C. A. Mirkin, R. L. Letsinger, R. C. Mucic, and J. J. Storhoff, *Nature*, **1996**, *382*, 607.
4. K. Sato, K. Hosokawa, and M. Maeda, *J. Am. Chem. Soc.*, **2003**, *125*, 8102.
5. H. Shiigi, S. Tokonami, H. Yakabe, and T. Nagaoka, *J. Am. Chem. Soc*., **2005**, *127*, 3280.
6. G. Braun, S. Joon, M. Dante, T.-Q. Nguyen, M. Moskovits, and N. Reich, *J. Am. Chem. Soc*., **2007**, *129*, 6387.
7. H. Du, C. M. Strohsahl, J. Camera, B. L. Miller, and T. D. Krauss, *J. Am. Chem. Soc*., **2005**, *127*, 7932.
8. C.-Y. Zhang, H.-C. Yeh, M. T. Kuroki, and Z.-H. Wang, *Nat. Mater.*, **2005**, *4*, 826.
9. T. Ihara, Y. Chokaura, S. Tanaka, and A. Jyo, *Chem. Commun*., **2002**, 2152.
10. R. Möller, A. Csáki, J. M. Köhler, and W. Fritzsche, *Nucleic Acids Res*., **2000**, *28*, e91.
11. K. Nakano, K. Doi, K. Tamura, Y. Katsumi, and M. Tazaki, *Chem. Commun*., **2003**, 1544.
12. K. Nakano, T. Yoshitake, Y. Yamashita, and E. F. Bowden, *Langmuir*, **2007**, *23*, 6270.
13. K. Nakano, H. Matsunaga, K. Sai, N. Soh, and T. Imato, *Anal. Chim. Acta*, **2006**, *578*, 93.
14. M. Maeda, Y. Mitsuhashi, K. Nakano, and M. Takagi, *Anal. Sci*., **1992**, *8*, 83.
15. C. Bustamante, J. Vesenka, C. L. Tang, W. Rees, M. Guthold, and R. Keller, *Biochemistry*, **1992**, *31*, 22.
16. R. C. Ebersole, J. A. Miller, J. R. Moran, and M. D. Ward, *J. Am. Chem. Soc*., **1990**, *112*, 3239.
17. P. W. K. Rothemund, *Nature*, **2006**, *440*, 297.
18. S. Nakagami, H. Matsunaga, K. Miyoshi, and A. Yamane, *Anal. Biochem*., **1991**, *192*, 11.
19. P. Lizard, X. Huang, A. Zhu, P. Bray-Ward, and D. C. Thomas, *Nat. Genet.*, **1998**, *19*, 225.
20. M. Falkenberg, P. Elias, and I. R. Lehman, *J. Biol. Chem*., **1998**, *273*, 32154.